




ARTICLE

Translational Therapeutics

Exploiting the reactive oxygen species imbalance in high-risk paediatric acute lymphoblastic leukaemia through auranofin

Mawar Karsa^{1,2}, Angelika Kosciolk^{1,2}, Angelika Bongers^{1,2}, Anna Mariana^{1,2,3}, Tim Failes^{1,2,3}, Andrew J. Gifford^{1,2,4}, Ursula R. Kees⁵, Laurence C. Cheung^{5,6}, Rishi S. Kotecha^{5,6,7,8}, Greg M. Arndt^{1,2,3}, Michelle Haber^{1,2}, Murray D. Norris^{1,2,9}, Rosemary Sutton^{1,2}, Richard B. Lock^{1,2,9}, Michelle J. Henderson^{1,2}  and Klaartje Somers^{1,2}

BACKGROUND: The prognosis for high-risk childhood acute leukaemias remains dismal and established treatment protocols often cause long-term side effects in survivors. This study aims to identify more effective and safer therapeutics for these patients.

METHODS: A high-throughput phenotypic screen of a library of 3707 approved drugs and pharmacologically active compounds was performed to identify compounds with selective cytotoxicity against leukaemia cells followed by further preclinical evaluation in patient-derived xenograft models.

RESULTS: Auranofin, an FDA-approved agent for the treatment of rheumatoid arthritis, was identified as exerting selective anti-cancer activity against leukaemia cells, including patient-derived xenograft cells from children with high-risk ALL, versus solid tumour and non-cancerous cells. It induced apoptosis in leukaemia cells by increasing reactive oxygen species (ROS) and potentiated the activity of the chemotherapeutic cytarabine against highly aggressive models of infant MLL-rearranged ALL by enhancing DNA damage accumulation. The enhanced sensitivity of leukaemia cells towards auranofin was associated with lower basal levels of the antioxidant glutathione and higher baseline ROS levels compared to solid tumour cells.

CONCLUSIONS: Our study highlights auranofin as a well-tolerated drug candidate for high-risk paediatric leukaemias that warrants further preclinical investigation for application in high-risk paediatric and adult acute leukaemias.

British Journal of Cancer (2021) 125:55–64; <https://doi.org/10.1038/s41416-021-01332-x>

BACKGROUND

Acute lymphoblastic leukaemia (ALL) is the most prevalent paediatric cancer, accounting for 25% of all malignancies in children below 15 years old.¹ Over the past five decades, clinical outcome of this once fatal disease has improved dramatically due to the implementation of risk stratification and risk-directed therapy.^{1,2} Nevertheless, the outcome for children with high-risk ALL, such as mixed-lineage leukaemia (MLL/KMT2A)-rearranged, Philadelphia chromosome-positive (Ph+) and early T-cell precursor ALL, is still relatively poor despite intensified therapies.^{3,4} In addition, the chemotherapeutics used in the current treatment regimens often cause serious short- and long-term side effects that impact quality of life, such as cardiotoxicity^{5–8} and abnormal physical growth rates.^{9,10} Novel, more potent therapeutic approaches are thus urgently needed and with an increasing number of children and adolescents cured of ALL, new therapeutic strategies for high-risk paediatric ALL should ideally be more cancer-selective to allow dose-reduction of conventional chemotherapeutics for the development of safer treatment

regimens. This is particularly relevant for patients who develop leukaemia before the age of one, in infancy. Infant ALL is in 80% of cases driven by a chromosomal rearrangement of the *MLL/KMT2A* gene, which results in an extremely aggressive and poor outcome leukaemia subtype.¹¹ Despite decades of clinical trials focused on optimising treatment schemes to increase survival rates for infant ALL, more than half of the patients still die within 5 years of diagnosis indicating that currently established treatment approaches have reached their limit and novel therapies are critically needed.^{11,12}

Drug repositioning or repurposing is one of the more recently developed strategies applied in drug discovery to overcome some of the major hurdles of the traditional drug discovery approach, namely the low success rates and the long timeline for approval of a new drug. The terminology refers to the identification of new therapeutics from a pool of existing drugs for application in the treatment of diseases other than those for which they were originally intended. This can be a very efficient approach to drug discovery as these drugs have established formulation and

¹Children's Cancer Institute, Lowy Cancer Research Centre, UNSW Sydney, Sydney, NSW, Australia; ²School of Women's and Children's Health, UNSW Sydney, Sydney, NSW, Australia; ³AACRF Drug Discovery Centre for Childhood Cancer, Children's Cancer Institute, Lowy Cancer Research Centre, UNSW Sydney, Sydney, NSW, Australia; ⁴Department of Anatomical Pathology, Prince of Wales Hospital, Randwick, NSW, Australia; ⁵Division of Children's Leukaemia and Cancer Research, Telethon Kids Cancer Centre, Telethon Kids Institute, University of Western Australia, Perth, WA, Australia; ⁶School of Pharmacy and Biomedical Sciences, Curtin University, Perth, WA, Australia; ⁷Department of Haematology and Oncology, Perth Children's Hospital, Perth, WA, Australia; ⁸Division of Paediatrics, School of Medicine, University of Western Australia, Perth, WA, Australia and ⁹UNSW Centre for Childhood Cancer Research, UNSW Sydney, Sydney, NSW, Australia

Correspondence: Michelle J. Henderson (mhenderson@ccia.unsw.edu.au)

These authors contributed equally: Michelle J. Henderson, Klaartje Somers

Received: 29 January 2020 Revised: 31 January 2021 Accepted: 19 February 2021

Published online: 9 April 2021

manufacturing methods, extensive data regarding in vivo absorption, distribution, metabolism, excretion and toxicity (ADMET), as well as clinical trial safety endpoint and post-marketing surveillance safety.¹³ Through bypassing time-consuming development, optimisation and ADMET steps, the drug discovery timeline could be reduced to 3–12 years compared to the conventional drug discovery pipeline which typically takes 10–17 years with a less than 10% probability of success.¹⁴

In this study, we applied a drug repurposing approach to identify novel and safer therapeutic options for paediatric high-risk ALL. We performed a cell-based high-throughput screen on a library of approved drugs and pharmacologically active compounds, discovering auranofin, an FDA-approved drug for the treatment of rheumatoid arthritis, as having strong anti-leukaemic effects in high-risk paediatric ALL.

METHODS

Cell lines and patient-derived xenograft cells

The panels of cell lines and patient-derived xenograft (PDX) cells used in this study are described in Supplementary Tables 1 and 2, respectively. All cell lines were authenticated and mycoplasma free.

High-throughput phenotypic screening

The following chemical libraries were used in the screening: Prestwick Chemical Library (Prestwick Chemical PC SAS, France), LOPAC®1280 library (Sigma-Aldrich, Australia), Tocriscreen Plus library (Tocris Bioscience, UK) and Selleck Inhibitor Library (Selleck Chemicals, USA), together combining 3707 compounds. Cell lines derived from high-risk ALL patients, PER-485 and CCRF-CEM (CEM) were seeded into 384-well culture plates. Test compounds were added to the assay plates for a final concentration of 5 μ M (in DMSO stock). Plates were incubated for 72 h at 37 °C, 5% CO₂. Resazurin was added and plates were incubated for 7 h. The difference in relative fluorescence units at time zero and 7 h of resazurin incubation was calculated for each well. The percentage cell viability for each test compound was calculated relative to the cells treated with vehicle (100% viability).

Cytotoxicity, synergy and in vitro cell-based assays

The cytotoxicity of drugs was assessed through resazurin-based assays and the inhibitory concentrations resulting in 50% reduction of cell survival relative to control (IC₅₀) values were calculated as previously described.^{15–17} In synergy studies, cells were exposed to a dilution series of compounds, as single agents or in combination at fixed ratios, in resazurin-based assays (72 h). The occurrence of synergy was determined with the Bliss Independence model.^{18,19} Bliss Prediction curves indicate the predicted % viability of the cells when exposed to the combination of compounds if both compounds work additively together. Synergy is visualised as the presence of a lower cell viability upon combination of two compounds compared to the viability predicted based on the presence of an additive effect of the compounds (i.e. the viability curve of the combination runs below the Bliss Prediction curve). Excess over Bliss (EOB) was calculated by determining the difference between the experimental fraction of cells affected by the combination of compounds and expected fractional inhibition of the combinations of compounds.²⁰ Synergy corresponds to EOB > 0, an additive effect to EOB = 0 and an antagonistic effect is represented by EOB < 0. Individual EOB values across all dose combination points used in the combination assays were summed to rank combination effects. Synergy corresponds to EOB (sum) > 0, an additive effect to EOB (sum) = 0 and an antagonistic effect is represented by EOB (sum) < 0. Observed synergies were further confirmed in a two-way 6 × 6 matrix synergy assay evaluating synergy over a broader concentration range and 36 concentration points. Synergy was scored based on the Bliss independence model and visualised by

Combeneft.²¹ The percentage of apoptotic cells was assessed by Annexin V and 7-Aminoactinomycin D (7-AAD) (BD Biosciences, Australia) flow cytometry as previously described.¹⁵

Reactive oxygen species assay

Reactive oxygen species (ROS) levels were determined by flow cytometry. Treated cells were stained with 2',7'-dichlorofluorescein diacetate (DCFDA) (Sigma-Aldrich, Australia) according to the manufacturer's instructions and samples were analysed on a FACSCalibur (BD Biosciences, Australia). The mean fluorescence intensity (MFI) of treated samples was calculated using FlowJo (Becton, Dickinson & Company, USA) relative to vehicle-treated cells.

Glutathione assay

The levels of glutathione in reduced (GSH) and oxidised (GSSG) states were determined through GSH recycling assays as previously described.^{22,23} GSH levels were calculated by subtracting GSSG values from total glutathione and normalising to protein content.

Protein analysis and immunoblotting

Methods for protein analysis and immunoblotting were described previously.^{17,24} Membranes were probed with antibodies described in Supplementary Table 3. Densitometry was performed using Image Lab 5.2.1 software (Bio-Rad, USA).

In vivo efficacy assessment in PDX models

All experimental studies were conducted with approval from the Animal Care and Ethics Committee of the University of New South Wales (Sydney, Australia) and in accordance to the New South Wales Animal Research Act 1985. Animals were housed in groups of four in 391 × 199 × 160 mm IVC GM500 cages (Tecniplast UK) with access to food and water. Environmental conditions were a temperature of 20–22 °C, humidity of 55–70% and 12-h light (from 0700) and 12-h dark cycle (from 1900). Animals were monitored twice daily and weighed weekly. At the start of the experiment, the animals weighed 18.64 ± 1.142 g (mean ± SD).

The used PDX cells are paediatric ALL patient-derived cells that have been serially passaged in immunodeficient mice and were generated as previously described.²⁵ For efficacy testing, PDX cells were inoculated into 6–9 week old female, immune-deficient NOD/SCID (NOD.CB17-Prkdc^{scid}/SzJ) mice (Animal Resources Centre, WA, Australia) and leukaemia engraftment was monitored weekly by assessing the percentage of human CD45-positive (huCD45⁺) cells in the peripheral blood as previously described.^{17,24} Mice were randomised into four groups when the median % huCD45⁺ cells exceeded 1% (8 mice per group): (i) vehicle control, (ii) 2.5–3.5 mg/kg auranofin (iii) 25 mg/kg cytarabine and (iv) 2.5–3.5 mg/kg auranofin plus 25 mg/kg cytarabine. Using groups of 8 mice, this PDX model is sensitive enough to detect less than a 2-fold difference in survival between control and treated mice with a probability of 90% and a significance of < 0.05. No blinding was done. Drugs were given via intraperitoneal injection for up to 3 cycles (5 days on, 2 days off). Dosing schemes were chosen based on maximal tolerated dose studies in NOD/SCID mice described in detail in the Supplementary Information and Supplementary Fig. 1 and entailed the use of doses achievable in humans. Auranofin was dissolved in 10% DMSO, 30% cremophor, 60% saline and cytarabine in saline. Once the huCD45⁺ cells in the peripheral blood reached 25% as a proportion of total human and murine CD45⁺ cells (event), mice were humanely sacrificed by CO₂ asphyxiation (without anaesthesia). Event-free survival (EFS) was graphically represented by Kaplan–Meier analysis and survival curves were compared by log-rank tests. To evaluate interactions between drugs in vivo, if the median EFS of mice treated with the drug combination was significantly greater than those induced by both single agents as

determined by Mantel–Cox test, this was defined as therapeutic enhancement. Any mouse that is not determined to be an event at the time of death is excluded from analysis.

Statistical analyses

GraphPad Prism 7.02 (GraphPad Software, San Diego, CA, USA) was used for all analyses. One sample *t*-tests or *t*-tests were used to assess the statistical significance of differences in measurements between two groups. One-way ANOVA with Tukey's correction for multiple comparisons was used for analyses involving three or more groups. *P*-values below 0.05 were considered statistically significant. No calculations were performed prior to the *in vitro* studies to determine the sample size of cell lines or PDXs as there was no prior knowledge of effect sizes.

RESULTS

A phenotypic screen of 3707 FDA-approved and drug-like compounds identifies auranofin as a novel candidate compound against high-risk paediatric ALL

To identify novel compounds targeting high-risk paediatric ALL, a primary phenotypic high-throughput screen was performed with a library containing 3707 compounds approved by the FDA or other agencies and/or pharmacologically active compounds. This library was firstly screened against two paediatric leukaemia cell lines derived from high-risk patients, namely the PER-485 cell line, derived from a relapsed infant MLL-r ALL patient,²⁶ and CCRF-CEM (CEM), a childhood relapsed T-cell ALL cell line. Cytotoxicity assays yielded 184 hit compounds that reduced the viability of both cell lines to below 10% (i.e. >90% growth inhibition) after a 72 h treatment with 5 μ M of each compound. Hit compounds were then subjected to a secondary screen against both cell lines used in the initial screen at lower concentrations (2, 1, 0.5 and 0.25 μ M) to select the most potent inhibitors (Fig. 1a). Out of the 184 compounds, 28 had an IC_{50} below 0.25 μ M against both cell lines. These 28 compounds (Fig. 1b), included microtubule inhibitors, anti-metabolites, DNA intercalators and proteasome inhibitors, several of which are currently in clinical use for paediatric ALL (e.g. vincristine, daunorubicin, bortezomib),¹² thereby validating that the screening approach was able to yield drugs that are effective against paediatric ALL. Other hits constituted compounds previously reported to be active *in vitro* or in preclinical models of various types of cancers such as SN38, the active metabolite of irinotecan, an analogue of camptothecin previously tested in refractory or relapsed leukaemia in children and adolescents (Fig. 1b).²⁷

To further select for compounds with specific cytotoxicity against high-risk paediatric leukaemia without affecting non-cancerous cells, these 28 compounds were subsequently evaluated in a full-dose–response screen against a non-malignant human lung fibroblast cell line, MRC-5 and an additional infant MLL-r ALL cell line (KOPN-8), in addition to the leukaemia cell lines used in the primary screen, PER-485 and CEM. For 10 out of 28 compounds, the IC_{50} for MRC-5 cells was at least 2-fold higher than the IC_{50} obtained for each of the leukaemia cell lines. Nine out of these compounds belonged to the drug classes of microtubule inhibitors, DNA intercalating agents/topoisomerase inhibitors, proteasome inhibitors or anti-metabolites. Representatives of these drug classes are either part of conventional treatment schemes for paediatric ALL (vincristine and daunorubicin;^{1,28} mitoxantrone (UK ALLR3,²⁹ Interfant-06)¹²), are currently in clinical trials for paediatric leukaemia (clofarabine (NHL16: NCT01451515)³⁰); bortezomib (IntReALLHR: NCT03590171; AIEOP-BFM ALL 2017: NCT03643276; TACL: NCT00440726)³¹) or were previously investigated in clinical trial for their use in paediatric ALL treatment (topotecan (NCT00187083)³²). Disulfiram, an FDA-approved drug for the treatment of alcoholism, has been shown to have cytotoxicity in ALL cells *in vitro*³³ and *in vivo*.³⁴ The remaining compound,

auranofin, an FDA-approved drug for the treatment of rheumatoid arthritis, has not been tested before as an agent against paediatric acute leukaemias and was therefore chosen for further evaluation.

Auranofin displays selective cytotoxicity against acute leukaemia cells

To further characterise the cytotoxic activity of auranofin against acute leukaemia, the compound was tested in cytotoxicity assays against a panel of 22 cancer cell lines and two non-malignant cell lines. The cancer cell line panel comprised 15 acute leukaemia cell lines, including cell lines derived from high-risk paediatric leukaemia (e.g. infant MLL-r ALL and acute myeloid leukaemia (AML), relapsed T-cell ALL) and seven solid tumour cell lines. Auranofin at 1 μ M reduced the viability of 15 out of 15 (100%) leukaemia cell lines below 40%, while only 1 out of 7 (14.3%) solid cancers and neither of the non-malignant cells was affected (Fig. 2a). Auranofin exhibited high cytotoxic activity against leukaemia cell lines with an average IC_{50} of 359 nM (range: 78–889 nM) (Supplementary Table 4) compared to 2288 nM for solid tumours and normal cell lines (range: 0.55–5 μ M) (Supplementary Table 4). The mean viability of the leukaemia cell lines at 1 μ M auranofin was significantly lower than the viability of the solid tumour cell lines ($p < 0.0001$) and non-malignant cells ($p < 0.0001$) indicating a selectivity of the compound for leukaemia cells (Fig. 2b). Even though the MLL-r leukaemia cells were amongst the most sensitive cell lines to auranofin, the mean IC_{50} values of MLL-r versus MLL-wt leukaemia cell lines in our panel were not significantly different (Supplementary Fig. 2A). Also, no significant difference was noted between the IC_{50} values of ALL versus AML cell lines (Supplementary Fig. 2B).

To investigate the mechanism by which auranofin reduced the viability of leukaemia cells, the level of apoptosis was measured by Annexin V staining in two treated MLL-r leukaemia cell lines, PER-485 and RS4;11. A significant increase in the percentage of apoptotic cells was seen as early as after 6 h of auranofin treatment with the proportion of apoptotic cells increasing over time (Fig. 2c). To further confirm apoptotic cell death, the level of cleaved PARP (an apoptotic marker) was examined. In concordance with the Annexin V data, treatment with auranofin induced PARP cleavage in the leukaemia cells within 6 h of treatment (Fig. 2c).

Auranofin rapidly kills leukaemia cells by ROS induction

Auranofin has been reported to increase ROS levels in cancer cells.^{35,36} To determine if the compound induced apoptosis in leukaemia cells through ROS induction, the level of intracellular ROS was measured in treated MLL-r leukaemia cell lines by flow cytometric analysis of cell permeate DCFDA. Within one hour of treatment, auranofin significantly increased levels of ROS in both cell lines and pre-treatment with a ROS scavenger, N-acetyl cysteine (NAC) prevented the increase of intracellular ROS (Fig. 3a). To further confirm the ROS-inducing action of auranofin, we assessed the occurrence of downstream effects of ROS, including increased expression of nuclear factor (erythroid-derived 2)-like 2 (Nrf2, a master regulator of the antioxidant response) and heme oxygenase 1 (HMOX1, a protein encoded by the Nrf2-activated *HMOX1* gene), as well as accumulation of DNA damage as shown by increased levels of phosphorylated histone H2A (γ H2AX). Auranofin increased the levels of Nrf2, HMOX1 and γ H2AX in leukaemia cells within 6 h and pre-treatment with NAC largely prevented these effects (Fig. 3b).

To further confirm that the auranofin-induced ROS increase was responsible for the apoptosis brought about by the compound, Annexin V levels were assessed in auranofin-treated leukaemia cells after pre-treatment with NAC. Pre-treatment with NAC almost completely prevented the auranofin-induced increase in proportion of apoptotic cells at 24 h (Fig. 3c), indicating that the cell death caused by auranofin in leukaemia cells is largely mediated through oxidative stress.

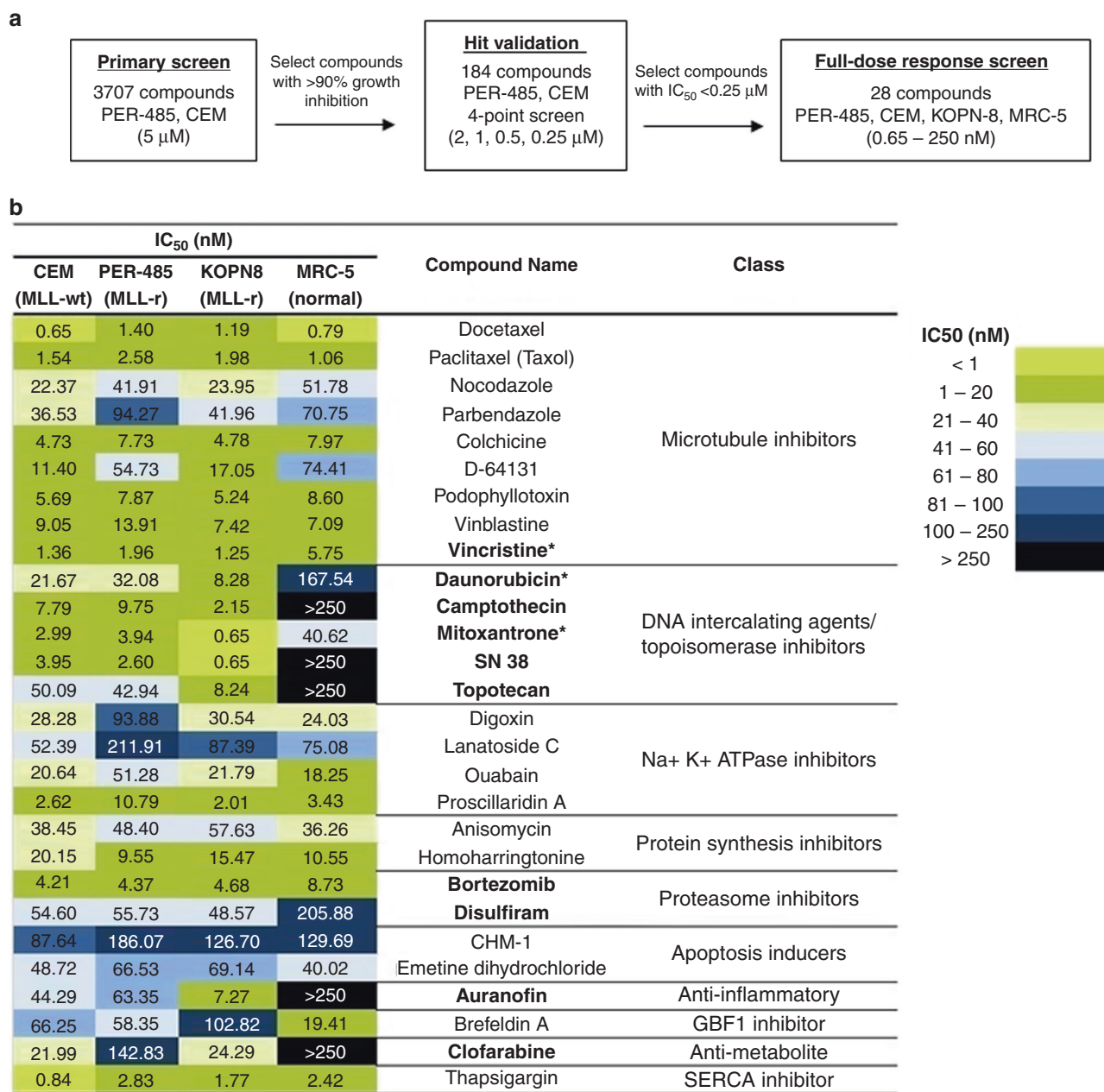


Fig. 1 Screening a library of 3707 approved drugs and pharmacologically active compounds to identify novel candidate drugs for high-risk paediatric leukaemia. **a** Schematic outline of the applied high-throughput screening approach. **b** Results of the characterisation of the 28 selected hit compounds by performing full dose–response cytotoxicity testing in three paediatric leukaemia and one non-malignant cell lines. Cell viability was determined after a 72 h drug exposure. The heat map displays the concentration with 50% cell growth reduction (IC₅₀) according to the colour key. Ten out of 28 compounds demonstrated lower toxicity to non-malignant cells than to the leukaemia cell lines (bolded), including conventional drugs that are currently used in standard therapy of paediatric ALL, vincristine, daunorubicin and mitoxantrone (marked with *).

Leukaemia cell lines show higher basal ROS and lower basal GSH levels compared to solid tumour cell lines

Our viability studies showed that auranofin displayed selective cytotoxic activity against acute leukaemia cells versus solid tumour cell lines. As auranofin exerts its leukaemia cell-killing effect through inducing ROS, we next compared basal ROS levels of cell lines derived from leukaemia versus solid tumours to gain more insight into the basis of this observed leukaemia selectivity of the drug. Significantly higher basal ROS levels were observed in leukaemia cell lines compared to solid tumour cell lines ($p = 0.0038$) (Fig. 3d). Based on these findings, we subsequently assessed the intracellular levels of glutathione (GSH), a master

antioxidant that plays a crucial role in scavenging ROS, regulating ROS levels and protecting cellular components from damage caused by ROS.³⁷ Leukaemia cell lines had significantly lower basal GSH levels compared to solid tumour cell lines ($p = 0.0140$), providing a possible explanation as to why auranofin displays selective cytotoxicity towards leukaemia cells (Fig. 3d).

Auranofin reduces the viability of PDX cells derived from paediatric high-risk ALL patients

To gain more evidence for the cytotoxic effects of auranofin against high-risk paediatric leukaemia, the compound was tested ex vivo against a panel of PDX cells derived from patients with

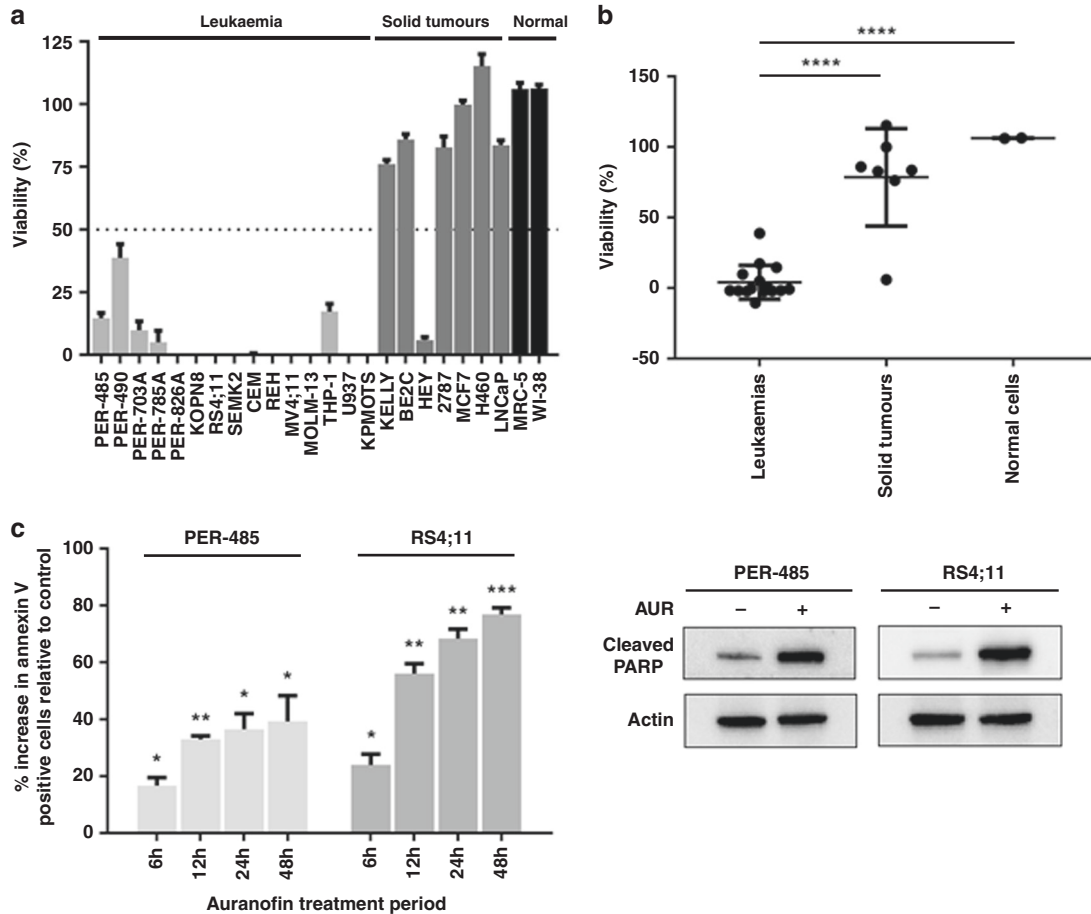


Fig. 2 Auranofin reduces the viability of acute leukaemia cells by inducing apoptosis. **a** Viability of a cell line panel after a 72 h treatment with 1 μ M of auranofin as measured in resazurin-based cytotoxicity assay relative to vehicle-treated cells. The bar graph presents the mean viability \pm SEM of three independent experiments. **b** Comparison of cell viability between leukaemia, solid tumour and non-malignant cell lines at 1 μ M auranofin. Dots represent the mean viability of a cell line (three independent experiments). Mean viability percentages between groups were compared by one-way ANOVA with Tukey's correction for multiple comparisons. **c** Flow cytometric analysis of Annexin V staining after 6–48 h drug treatment with auranofin at 600 nM. For each timepoint, apoptosis is expressed as the percentage increase in Annexin V positive cells relative to vehicle-treated control (0%). The bar graph presents the mean increase in percentage of Annexin V positive cells \pm SEM of three independent experiments. For each time point, one-sample *t*-tests were used to determine the statistical significance of the % increases relative to vehicle. A representative immunoblot analysis of cleaved PARP protein levels in sensitive MLL-r leukaemia cell lines following 6 h of auranofin (AUR) treatment (600 nM) is shown. Total actin was used as a loading control. Western blotting was performed at least two times in independent experiments. In all statistical analyses, asterisks represent significance levels of *P*-values. **P* < 0.05; ***P* < 0.01; ****P* < 0.001; *****P* < 0.0001.

high-risk (MLL-r infant ALL, Ph+ ALL, Ph-like ALL and T-ALL subtypes) or poor outcome disease. These PDXs have previously been shown to retain the immunophenotypic and genotypic characteristics of the original disease, with their *in vivo* responses to established chemotherapeutics correlating tightly with the clinical outcome of the respective donor patients.^{38,39}

Auranofin showed potent *in vitro* cytotoxic activity against PDX cells derived from some of the most aggressive subtypes of paediatric ALL and similarly to the leukaemia cell lines, auranofin decreased the viability of ALL PDX cells with IC₅₀ values ranging from 55 to 1597 nM (Table 1; Supplementary Fig. 3A, B, average IC₅₀ \pm SD = 331 \pm 407 nM). The most sensitive PDXs were characterised by the presence of an MLL-rearrangement but the mean achieved IC₅₀ values were not significantly different between MLL-r and MLL-wt PDX cells (Supplementary Fig. 2C).

To determine if the compound also increased intracellular ROS levels in ALL PDX cells, the level of intracellular ROS was measured in treated and untreated ALL PDX cells by flow cytometric analysis of cell permeate DCFDA. In concordance with the cell line data, across the PDX panel, auranofin-treated PDX cells had higher ROS levels than untreated PDX cells (Supplementary Fig. 3C).

Auranofin synergises with conventional agents against high-risk paediatric ALL

To investigate whether auranofin is able to enhance the activity of conventional agents used in high-risk paediatric acute leukaemia treatment, *in vitro* synergy assays were performed in three leukaemia cell lines (PER-485, PER-490 and RS4;11), combining auranofin with each of nine chemotherapeutic compounds (cytarabine, mitoxantrone, daunorubicin, etoposide, topotecan, methotrexate, prednisolone, vincristine or *L*-asparaginase) used in the treatment of paediatric acute leukaemia. Synergy, defined as an Excess over Bliss (EOB) value > 0, was observed between auranofin and cytarabine, prednisolone or *L*-asparaginase in the PER-485 and PER-490 cell lines, between auranofin and mitoxantrone in the PER-490 and RS4;11 cells, between auranofin and etoposide in the PER-490 cells and between auranofin and daunorubicin or topotecan in the RS4;11 cell line (Fig. 4a, Supplementary Fig. 4). The observed synergy between auranofin and cytarabine, prednisolone or *L*-asparaginase was further confirmed over broader concentration ranges and more dose combination points in 6 \times 6 matrix synergy assays (Supplementary Fig. 5).

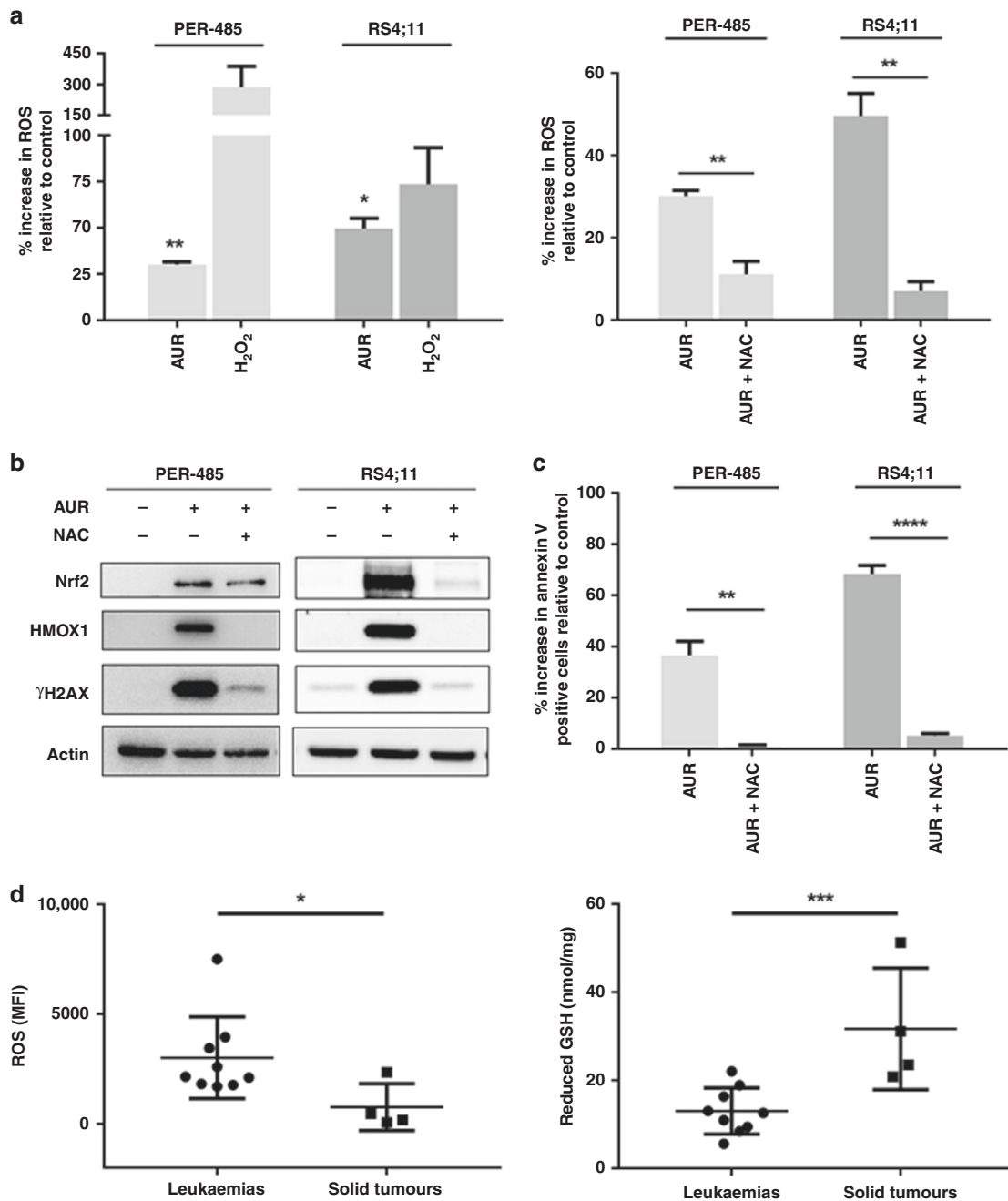


Fig. 3 Auranofin induces apoptosis in acute leukaemia cells by inducing ROS. **a** Increase in intracellular reactive oxygen species (ROS) levels compared to vehicle-treated control (0%) as measured by flow cytometric analysis of DCFDA after a 1 h auranofin (AUR) treatment (600 nM) without (left panel) or with pre-incubation with 5 mM of ROS scavenger, N-acetyl cysteine (NAC) (right panel). Fifteen-minute 500 μM hydrogen peroxide (H₂O₂) treatment was conducted alongside as a positive control (left panel). Bar graphs represent mean values measured ± SEM of three independent experiments. One-sample *t*-tests were used to determine the statistical significance of the mean % increase in ROS relative to vehicle in the left panel, while mean % increases between auranofin-treated and NAC pre-treated groups (right panel) were compared by *t*-tests. **b** A representative immunoblot analysis of Nrf2, HMOX1 and γH2AX expression levels upon 6 h treatment with AUR with and without pre-treatment with NAC. Total actin was used as a loading control. Western blotting was performed at least two times in independent experiments. **c** Impact of NAC pre-treatment on apoptosis induction by auranofin at 24 h as measured by Annexin V staining. The apoptosis results are expressed as the mean ± SEM of three independent experiments. *t*-tests were used to compare relative increases in Annexin V positive cells in treated cells. **d** Basal levels of ROS (left panel) and glutathione (GSH, right panel) in leukaemia and solid tumour cell lines, measured as mean fluorescence intensity (MFI) by flow cytometric analysis of DCFDA and by an enzymatic recycling spectrophotometric assay, respectively. Dots represent mean cellular MFI or GSH values of three replicates. Error bars represent SEM of three independent experiments. Means between groups were compared by *t*-tests. In all statistical analyses, asterisks represent significance levels of *P*-values. **P* < 0.05; ***P* < 0.01; *****P* < 0.0001.

Table 1. Cytotoxicity of auranofin against a panel of xenograft cells derived from children with high-risk paediatric ALL.

Lineage	Xenograft	Disease status at biopsy	IC ₅₀ (nM)
MLL-r ALL	MLL-2	Diagnosis	377
	MLL-5	Diagnosis	132
	MLL-6	Diagnosis	389
	MLL-7	Diagnosis	79
	MLL-8	Diagnosis	55
	MLL-14	Diagnosis	122
B-ALL	ALL-2	Third relapse	208
	ALL-7	Diagnosis	154
	ALL-19	Relapse	184
Philadelphia + ALL	ALL-4	Diagnosis	119
	ALL-55	Diagnosis	353
Philadelphia-like ALL	PAKSWW	Diagnosis	127
T-ALL	ALL-8	Relapse	1597
	ALL-31	Diagnosis	744

Clinical trials often adhere to the current standard induction regimens because they are well established, effective in many patients and used in patient minimal residual disease (MRD) stratification. Therefore, if auranofin was to enter a clinical trial, it would be highly likely to be combined with post-induction chemotherapy drugs rather than induction drugs. Cytarabine was, therefore, selected for further evaluation *in vivo* as the drug is used in most ALL treatment phases after induction therapy and demonstrated synergy with auranofin in two cytarabine-resistant infant MLL-r leukaemia cell lines. Cytarabine, a nucleoside analogue, exerts its anti-cancer function by incorporating into newly synthesised DNA, inducing DNA damage.⁴⁰ As ROS are known to induce DNA damage as well, we assessed whether the mechanism of synergy between auranofin and cytarabine was through the enhanced accumulation of DNA damage upon combination of these two drugs. An increase in γ H2AX was observed upon *in vitro* treatment of PER-485 and PER-490 cells with either auranofin or cytarabine as single agents. Combined treatment with both drugs strongly enhanced the level of γ H2AX even further, suggesting heightened DNA damage induction as a possible mechanism of the observed synergy between the two drugs (Fig. 4b, Supplementary Fig. 6).

Auranofin potentiates cytarabine in a therapy-resistant infant MLL-r ALL PDX model

We next investigated the capacity of auranofin to potentiate cytarabine *in vivo* using PDX models for high-risk paediatric ALL. NOD/SCID mice were inoculated with either of two infant MLL-r ALL PDXs, MLL-5 and MLL-7, and treated with auranofin, cytarabine or the drug combination for up to 3 weeks. Maximum tolerated dose studies were performed to determine well-tolerated doses and administered doses that are achievable in humans. The PDXs were selected for efficacy testing based on their relatively low IC₅₀ for auranofin *in vitro*. MLL-5 is a highly aggressive PDX that is resistant to conventional chemotherapies such as an induction-type regimen based on the use of vincristine, dexamethasone and *L*-asparaginase (VXL), while MLL-7 is more responsive to VXL.²⁵ While cytarabine and auranofin each administered individually had no significant effect compared to vehicle control in the MLL-5 PDX, the combination significantly delayed the increase in the level of circulating leukaemia cells (Fig. 4c). Therapeutic enhancement, defined as significantly greater activity for a drug combination than for either single agent,⁴¹ was observed for auranofin combined with cytarabine, with the combination significantly delaying

leukaemia progression and extending survival (Fig. 4b) compared to either single agent. However, in the MLL-7 PDX, auranofin provided no further enhancement over cytarabine, which alone already induced a significant leukaemia growth delay (Supplementary Fig. 7A, B). Despite the absence of an effect of the combination on leukaemia progression in this model, molecular analysis indicated increased accumulation of DNA damage in spleen cells harvested from treated mice at a time point before apoptosis was evident (no increase in the ratio of cleaved to total PARP) (Supplementary Fig. 7C), in analogy to the data generated *in vitro* for PER-485 and PER-490 cells (Fig. 4b, Supplementary Fig. 6). This indicates that, despite the absence of a therapeutic effect of the drug combination in the MLL-7 PDX, the drugs were applied at doses that exerted molecular effects, confirming target engagement.

DISCUSSION

Despite significant improvements in the treatment and outcome of childhood ALL, the prognosis for subgroups of high-risk patients remains dismal. The poor clinical outcome linked to high-risk disease and the limitations of treatment intensification urgently warrant the development of more effective and safer therapeutics. Here, we identified auranofin, a gold (I)-containing compound previously approved by the FDA for the treatment of rheumatoid arthritis, as a novel candidate drug against high-risk paediatric ALL. We showed that auranofin exhibited selective cytotoxic activity towards leukaemia cell lines and patient-derived xenograft cells by increasing intracellular ROS levels and that the drug demonstrated synergy with several conventional drugs used in the treatment of high-risk paediatric acute leukaemia. Auranofin potentiated cytarabine in a treatment-refractory infant MLL-r ALL PDX model through enhancing DNA damage accumulation in the leukaemic cells. Our study provides impetus for a further preclinical evaluation of auranofin for therapeutic application in paediatric and adult acute leukaemias.

Auranofin was originally used and approved for the treatment of rheumatoid arthritis based on its potential to suppress inflammation and slow down disease progression.^{42,43} With a well-known toxicity profile including mostly mild side effects,^{42,44} the compound was found to be safe for use in both adults and children.⁴⁴ Auranofin is currently investigated as a candidate treatment for a range of diseases including neurodegenerative disorders, HIV/AIDS, parasitic and bacterial infections, and cancer.⁴³ When administered either alone or in combination with other therapeutics, auranofin has been reported to inhibit tumour growth in animal models for breast,⁴⁵ colorectal⁴⁶ and lung⁴⁷ cancers, as well as several types of leukaemias, such as murine lymphocytic leukaemia,⁴⁸ chronic myelogenous leukaemia⁴⁹ and chronic lymphocytic leukaemia.³⁵ The current study is the first to report on the therapeutic efficacy of auranofin against preclinical models of high-risk paediatric ALL and its selectivity towards haematological cancer cells.

We show that auranofin causes leukaemic cell death through inducing increases in cellular ROS levels, which is consistent with auranofin's reported inhibitory action on redox enzymes.^{35,47} It is well established that cancer cells have higher intracellular ROS levels than normal cells, and this has resulted in the notion that cancer cells might be more sensitive to induced ROS increases and oxidative stress than healthy cells.⁵⁰ We found that leukaemia cell lines have higher basal levels of ROS and lower baseline GSH levels than solid cancer cell lines, providing an explanation for the observed selective activity of auranofin against leukaemia cell lines and potentially its selection from the screen. This is in line with reports from studies in leukaemia patients that revealed higher levels of oxidative stress-related parameters such as protein carbonylation and superoxide dismutase enzyme activities in blood of ALL patients compared to healthy controls,⁵¹ as well as in AML patients who relapsed compared to those who did not,

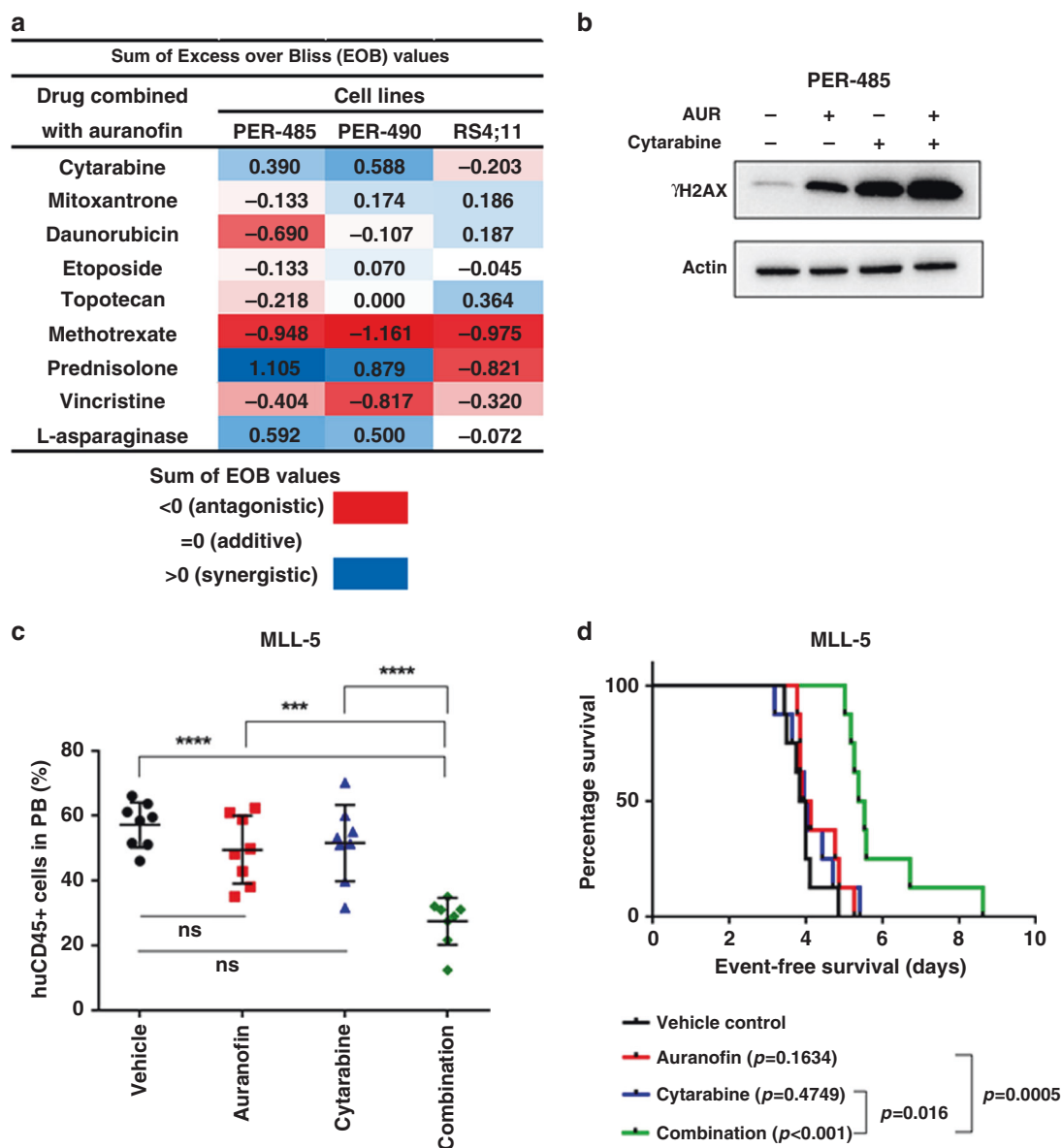


Fig. 4 The combination of auranofin and cytarabine induces a leukaemia growth delay in a highly chemo-resistant infant MLL-r ALL PDX. **a** Excess over Bliss (EOB) value of in vitro synergy assay of auranofin with 9 conventional agents in PER-485, PER-490 and RS4;11 cells. Cells were subjected to increasing doses of auranofin or chemotherapeutic alone, or a combination of the two simultaneously at fixed-ratios for 72 h, and viability was assessed using resazurin-based cytotoxicity assay and measured relative to vehicle-treated cells. EOB was calculated by determining, for each dose, the difference between the experimental fraction of cells affected by the combination of compounds and expected fractional inhibition of the combinations of compounds. EOB values across all tested concentrations were summed to rank combination effects. Synergy corresponds to EOB (sum) > 0, an additive effect to EOB (sum) = 0 and an antagonistic effect is represented by EOB (sum) < 0. The heat map displays the EOB sum according to the colour key. **b** Representative immunoblot of two independent experiments for γ H2AX levels in PER-485 leukaemia cells treated with each drug alone or in combination for 48 h. Auranofin (AUR) was added at 590 nM and cytarabine at 3.4 μ M. **c** Level of human CD45-positive cells (huCD45+) detected in peripheral blood (PB) at day 8 post treatment in MLL-5 mouse model. Mice were treated with (i) vehicle control (10% DMSO, 30% Cremophor, 60% saline), (ii) 2.5 mg/kg auranofin, (iii) 25 mg/kg cytarabine, or (iv) a combination of the drugs *via* intraperitoneal injection for up to three cycles (5 days on, 2 days off). Mean human CD45 percentages between groups were compared by one-way ANOVA with Tukey's correction for multiple comparisons. Asterisks represent significance levels of *P*-values. ***P* < 0.01; ****P* < 0.001; *****P* < 0.0001. **d** Kaplan–Meier survival curve of MLL-5 mouse model. Survival curves were compared by log-rank Mantel–Cox test.

suggesting a role for increased ROS levels in leukaemia progression.⁵² Our finding of selective targeting of leukaemia cells by auranofin through exploiting their higher baseline ROS levels suggests that there is a therapeutic window for this well-tolerated drug in leukaemia.

We observed that auranofin was able to potentiate the effects of cytarabine in our in vitro and in vivo models of high-risk paediatric ALL that were unresponsive to cytarabine as a single

agent. This constitutes a highly relevant finding that warrants further preclinical validation, particularly since these models were derived from infants with MLL-r ALL, which is the high-risk disease subtype with the worst outcome in paediatric ALL and represents a major challenge in paediatric oncology today. To further advance this drug towards testing in clinical trials for acute leukaemias, future studies should involve preclinical testing in an expanded panel of paediatric and adult leukaemia models

including other high-risk subtypes for which novel and safer treatments are urgently needed (e.g. T-ALL), as well as additional combination testing with other conventional drugs (e.g. corticosteroids). The testing of the drug in extended PDX panels will help shed light on markers that predict sensitivity to drug combinations, which is important for future patient selection in clinical trials. Furthermore, in a future preclinical assessment of auranofin for inclusion in treatment schemes for high-risk paediatric ALL, it would be interesting to include a detailed assessment of the effects of the drug on leukaemic blast numbers in the bone marrow, spleen and peripheral blood. Bioluminescent PDX mouse models of high-risk ALL that involve lentivirally transduced ALL PDX cells that stably express luciferase, for which the growth can be monitored through bioluminescence imaging, could be used for assessment of whole-body leukaemia burden.⁵³

In conclusion, our study highlights the potential of the drug repurposing approach to identify novel therapeutics for high-risk leukaemia and supports further preclinical evaluation of auranofin in combination with current chemotherapeutic regimens as a new approach for the treatment of infant MLL-r ALL and potentially other paediatric and adult high-risk acute leukaemia subtypes.

ACKNOWLEDGEMENTS

Patient samples and related clinical information for this study were kindly provided by Sydney Children's Tumour Bank Network. Children's Cancer Institute Australia is affiliated with UNSW Sydney and The Sydney Children's Hospitals Network.

AUTHOR CONTRIBUTIONS

M.K., A.K., A.B., A.M. and A.J.G. conducted the experiments and analysed the data; U.R. K., L.C.C. and R.S.K. provided guidance and access to the cell lines and patient material used in the study; K.S. and M.J.H. conceived the project and designed the experiments. T.F., G.M.A., M.H., M.D.N., R.S. and R.B.L. provided crucial suggestions and support with study design; M.K. wrote the manuscript under the guidance of K.S. and M.J.H. who critically reviewed the manuscript; All authors reviewed the manuscript.

ADDITIONAL INFORMATION

Ethics approval and consent to participate Animal studies were conducted with approval from the Animal Care and Ethics Committee of the University of New South Wales (Sydney, Australia).

Consent to publish Not applicable.

Data availability All data generated or analysed during this study are included in this published article and its Supplementary information files.

Competing interests The authors declare no competing interests.

Funding information This research was supported by grants from the Anthony Rothe Memorial Trust, the Cancer Council NSW, the Tenix Foundation, the Kids Cancer Alliance, the ISG Foundation, the National Health and Medical Research Council of Australia (NHMRC Fellowships APP1059804 and APP1157871) to R.B.L. and the Children's Leukaemia & Cancer Research Foundation (Perth, Western Australia) to U.R.K.

Supplementary information The online version contains supplementary material available at <https://doi.org/10.1038/s41416-021-01332-x>.

Publisher's note Springer Nature remains neutral with regard to jurisdictional claims in published maps and institutional affiliations.

REFERENCES

- Pui, C. H. in *Childhood Leukemias*. 3rd edn, Chapter 13, Acute lymphoblastic leukemia, 332–366 (Cambridge University Press, 2012).
- Pui, C. H., Yang, J. J., Hunger, S. P., Pieters, R., Schrappe, M., Biondi, A. et al. Childhood acute lymphoblastic leukemia: progress through collaboration. *J. Clin. Oncol.* **33**, 2938–2948 (2015).

- Coustan-Smith, E., Mullighan, C. G., Onciu, M., Behm, F. G., Raimondi, S. C., Pei, D. et al. Early T-cell precursor leukaemia: a subtype of very high-risk acute lymphoblastic leukaemia. *Lancet Oncol.* **10**, 147–156 (2009).
- Boer, J. M. & den Boer, M. L. BCR-ABL1-like acute lymphoblastic leukaemia: from bench to bedside. *Eur. J. Cancer* **82**, 203–218 (2017).
- Adams, M. J. & Lipshultz, S. E. Pathophysiology of anthracycline- and radiation-associated cardiomyopathies: implications for screening and prevention. *Pediatr. Blood Cancer* **44**, 600–606 (2005).
- Ness, K. K., Armenian, S. H., Kadan-Lottick, N. & Gurney, J. G. Adverse effects of treatment in childhood acute lymphoblastic leukemia: general overview and implications for long-term cardiac health. *Expert Rev. Hematol.* **4**, 185–197 (2011).
- Green, D. M., Kawashima, T., Stovall, M., Leisenring, W., Sklar, C. A., Mertens, A. C. et al. Fertility of female survivors of childhood cancer: a report from the childhood cancer survivor study. *J. Clin. Oncol.* **27**, 2677–2685 (2009).
- Green, D. M., Kawashima, T., Stovall, M., Leisenring, W., Sklar, C. A., Mertens, A. C. et al. Fertility of male survivors of childhood cancer: a report from the Childhood Cancer Survivor Study. *J. Clin. Oncol.* **28**, 332–339 (2010).
- Mody, R., Li, S., Dover, D. C., Sallan, S., Leisenring, W., Oeffinger, K. C. et al. Twenty-five-year follow-up among survivors of childhood acute lymphoblastic leukemia: a report from the Childhood Cancer Survivor Study. *Blood* **111**, 5515–5523 (2008).
- Robison, L. L. Late effects of acute lymphoblastic leukemia therapy in patients diagnosed at 0–20 years of age. *Hematology Am. Soc. Hematol. Educ. Program* **2011**, 238–242 (2011).
- Pieters, R., Schrappe, M., De Lorenzo, P., Hann, I., De Rossi, G., Felice, M. et al. A treatment protocol for infants younger than 1 year with acute lymphoblastic leukaemia (Interfant-99): an observational study and a multicentre randomised trial. *Lancet* **370**, 240–250 (2007).
- Kotecha, R. S., Gottardo, N. G., Kees, U. R. & Cole, C. H. The evolution of clinical trials for infant acute lymphoblastic leukemia. *Blood Cancer J.* **4**, e200 (2014).
- Li, Y. Y. & Jones, S. J. Drug repositioning for personalized medicine. *Genome Med.* **4**, 27 (2012).
- Ashburn, T. T. & Thor, K. B. Drug repositioning: identifying and developing new uses for existing drugs. *Nat. Rev. Drug Disco.* **3**, 673–683 (2004).
- Somers, K., Chudakova, D. A., Middlemiss, S. M. C., Wen, V. W., Clifton, M., Kwek, A. et al. CCI-007, a novel small molecule with cytotoxic activity against infant leukemia with MLL rearrangements. *Oncotarget* **7**, 46067–46087 (2016).
- Khaw, S. L., Suryani, S., Evans, K., Richmond, J., Robbins, A., Kurmasheva, R. T. et al. Venetoclax responses of pediatric ALL xenografts reveal sensitivity of MLL-rearranged leukemia. *Blood* **128**, 1382–1395 (2016).
- Somers, K., Wen, V. W., Middlemiss, S. M. C., Osborne, B., Forgham, H., Jung, M. et al. A novel small molecule that kills a subset of MLL-rearranged leukemia cells by inducing mitochondrial dysfunction. *Oncogene* **38**, 3824–3842 (2019).
- Bliss, C. I. The calculation of microbial assays. *Bacteriol. Rev.* **20**, 243–258 (1956).
- Zhao, W., Sachsenmeier, K., Zhang, L., Sult, E., Hollingsworth, R. E. & Yang, H. A new bliss independence model to analyze drug combination data. *J. Biomol. Screen* **19**, 817–821 (2014).
- Goswami, C. P., Cheng, L., Alexander, P. S., Singal, A. & Li, L. A new drug combinatory effect prediction algorithm on the cancer cell based on gene expression and dose-response curve. *Pharmacomet. Syst. Pharm.* **4**, e9 (2015).
- Di Veroli, G. Y., Fornari, C., Wang, D., Mollard, S., Bramhall, J. L., Richards, F. M. et al. Combeneft: an interactive platform for the analysis and visualization of drug combinations. *Bioinformatics* **32**, 2866–2868 (2016).
- Rahman, I., Kode, A. & Biswas, S. K. Assay for quantitative determination of glutathione and glutathione disulfide levels using enzymatic recycling method. *Nat. Protoc.* **1**, 3159–3165 (2006).
- Gana, C. C., Hanssen, K. M., Yu, D. M. T., Flemming, C. L., Wheatley, M. S., Conseil, G. et al. MRP1 modulators synergize with buthionine sulfoximine to exploit colateral sensitivity and selectively kill MRP1-expressing cancer cells. *Biochem. Pharm.* **168**, 237–248 (2019).
- Somers, K., Evans, K., Cheung, L., Karsa, M., Pritchard, T., Kosciolk, A. et al. Effective targeting of NAMPT in patient-derived xenograft models of high-risk pediatric acute lymphoblastic leukemia. *Leukemia*. **34**, 1524–1539 (2020).
- Richmond, J., Carol, H., Evans, K., High, L., Mendo, A., Robbins, A. et al. Effective targeting of the P53-MDM2 axis in preclinical models of infant MLL-rearranged acute lymphoblastic leukemia. *Clin. Cancer Res.* **21**, 1395–1405 (2015).
- Kees, U. R., Ford, J., Watson, M., Murch, A., Ringñer, M., Walker, R. J. et al. Gene expression profiles in a panel of childhood leukemia cell lines mirror critical features of the disease. *Mol. Cancer Ther.* **2**, 671–677 (2003).
- Saletta, F., Wadham, C., Ziegler, D. S., Marshall, G. M., Haber, M., McCowage, G. et al. Molecular profiling of childhood cancer: Biomarkers and novel therapies. *BBA Clin.* **1**, 59–77 (2014).
- Brown, P. Treatment of infant leukemias: challenge and promise. *Hematology Am. Soc. Hematol. Educ. Program* **2013**, 596–600 (2013).
- Parker, C., Waters, R., Leighton, C., Hancock, J., Sutton, R., Moorman, A. V. et al. Effect of mitoxantrone on outcome of children with first relapse of acute

- lymphoblastic leukaemia (ALL R3): an open-label randomised trial. *Lancet* **376**, 2009–2017 (2011).
30. Burkhardt, B., Mueller, S., Khanam, T. & Perkins, S. L. Current status and future directions of T-lymphoblastic lymphoma in children and adolescents. *Br. J. Haematol.* **173**, 545–559 (2016).
 31. Kuhlen, M., Klusmann, J.-H. & Hoell, J. I. Molecular approaches to treating pediatric leukemias. *Front Pediatr.* **7**, 356 (2019).
 32. Hijjiya, N., Stewart, C. F., Zhou, Y., Campana, D., Coustan-Smith, E., Rivera, G. K. et al. Phase II study of topotecan in combination with dexamethasone, asparaginase, and vincristine in pediatric patients with acute lymphoblastic leukemia in first relapse. *Cancer* **112**, 1983–1991 (2008).
 33. Conticello, C., Martinetti, D., Adamo, L., Buccheri, S., Giuffrida, R., Parrinello, N. et al. Disulfiram, an old drug with new potential therapeutic uses for human hematological malignancies. *Int. J. Cancer* **131**, 2197–2203 (2012).
 34. Deng, M., Jiang, Z., Li, Y., Zhou, Y., Li, J., Wang, X. et al. Effective elimination of adult B-lineage acute lymphoblastic leukemia by disulfiram/copper complex in vitro and in vivo in patient-derived xenograft models. *Oncotarget* **7**, 82200–82212 (2016).
 35. Fiskus, W., Saba, N., Shen, M., Ghias, M., Liu, J., Gupta, S. D. et al. Auranofin induces lethal oxidative and endoplasmic reticulum stress and exerts potent preclinical activity against chronic lymphocytic leukemia. *Cancer Res* **74**, 2520–2532 (2014).
 36. Hwang-Bo, H., Jeong, J. W., Han, M. H., Park, C., Hong, S. H., Kim, G. Y. et al. Auranofin, an inhibitor of thioredoxin reductase, induces apoptosis in hepatocellular carcinoma Hep3B cells by generation of reactive oxygen species. *Gen. Physiol. Biophys.* **36**, 117–128 (2017).
 37. Zitka, O., Skalickova, S., Gumulec, J., Masarik, M., Adam, V., Hubalek, J. et al. Redox status expressed as GSH:GSSG ratio as a marker for oxidative stress in paediatric tumour patients. *Oncol. Lett.* **4**, 1247–1253 (2012).
 38. Lock, R. B., Liem, N., Farnsworth, M. L., Milross, C. G., Xue, C., Tajbakhsh, M. et al. The nonobese diabetic/severe combined immunodeficient (NOD/SCID) mouse model of childhood acute lymphoblastic leukemia reveals intrinsic differences in biologic characteristics at diagnosis and relapse. *Blood* **99**, 4100–4108 (2002).
 39. Liem, N. L., Papa, R. A., Milross, C. G., Schmid, M. A., Tajbakhsh, M., Choi, S. et al. Characterization of childhood acute lymphoblastic leukemia xenograft models for the preclinical evaluation of new therapies. *Blood* **103**, 3905–3914 (2004).
 40. Geller, H. M., Cheng, K. Y., Goldsmith, N. K., Romero, A. A., Zhang, A. L., Morris, E. J. et al. Oxidative stress mediates neuronal DNA damage and apoptosis in response to cytosine arabinoside. *J. Neurochem* **78**, 265–275 (2001).
 41. Houghton, P. J., Morton, C. I., Gorlick, R., Lock, R. B., Carol, H., Reynolds, C. P. et al. Stage 2 combination testing of rapamycin with cytotoxic agents by the Pediatric preclinical testing program. *Mol. Cancer Ther.* **9**, 101–112 (2010).
 42. Cruickshank, M. N., Ford, J., Cheung, L. C., Heng, J., Singh, S., Wells, J. et al. Systematic chemical and molecular profiling of MLL-rearranged infant acute lymphoblastic leukemia reveals efficacy of romidepsin. *Leukemia* **31**, 40–50 (2017).
 43. Furst, D. E. Mechanism of action, pharmacology, clinical efficacy and side effects of auranofin. An orally administered organic gold compound for the treatment of rheumatoid arthritis. *Pharmacotherapy* **3**, 284–298 (1983).
 44. Roder, C. & Thomson, M. J. Auranofin: repurposing an old drug for a golden new age. *Drugs R. D.* **15**, 13–20 (2015).
 45. Kean, W. F. & Kean, I. R. Clinical pharmacology of gold. *Inflammopharmacology* **16**, 112–125 (2008).
 46. Liu, N., Li, X., Huang, H., Zhao, C., Liao, S., Yang, C. et al. Clinically used anti-rheumatic agent auranofin is a proteasomal deubiquitinase inhibitor and inhibits tumor growth. *Oncotarget* **5**, 5453–5471 (2014).
 47. Hrabe, J. E., O’Leary, B. R., Fath, M. A., Rodman, S. N., Button, A. M., Domann, F. E. et al. Disruption of thioredoxin metabolism enhances the toxicity of transforming growth factor β -activated kinase 1 (TAK1) inhibition in KRAS-mutated colon cancer cells. *Redox Biol.* **5**, 319–327 (2015).
 48. Fan, C., Zheng, W., Fu, X., Li, X., Wong, Y. S. & Chen, T. Enhancement of auranofin-induced lung cancer cell apoptosis by selenocystine, a natural inhibitor of TrxR1 in vitro and in vivo. *Cell Death Dis.* **5**, e1191 (2014).
 49. Simon, T. M., Kunishima, D. H., Vibert, G. J. & Lorber, A. Screening trial with the coordinated gold compound auranofin using mouse lymphocyte leukemia P388. *Cancer Res* **41**, 94–97 (1981).
 50. Chen, X., Shi, X., Zhao, C., Li, X., Lan, X., Liu, S. et al. Anti-rheumatic agent auranofin induced apoptosis in chronic myeloid leukemia cells resistant to imatinib through both Bcr/Abl-dependent and -independent mechanisms. *Oncotarget* **5**, 9118–9132 (2014).
 51. Lewandowski, D., Barroca, V., Ducongé, F., Bayer, J., Van Nhieu, J. T., Pestourie, C. et al. In vivo cellular imaging pinpoints the role of reactive oxygen species in the early steps of adult hematopoietic reconstitution. *Blood* **115**, 443–452 (2010).
 52. Battisti, V., Maders, L. D., Bagatini, M. D., Santos, K. F., Spanevello, R. M., Maldonado, P. A. et al. Measurement of oxidative stress and antioxidant status in acute lymphoblastic leukemia patients. *Clin. Biochem.* **41**, 511–518 (2008).
 53. Jones, L., Richmond, J., Evans, K., Carol, H., Jing, D., Kurmasheva, R. T. et al. Bioluminescence imaging enhances analysis of drug responses in a patient-derived xenograft model of pediatric ALL. *Clin. Cancer Res.* **23**, 3744–3755 (2017).